WIND TUNNEL PERFORATED WALL CORRECTIONS FOR THE ONERA M4R MODEL

Mihaela BURGHIU (MANEA)[1,2*], Corneliu Ioan STOICA[1] , Adrian BURGHIU[1,2]

Improving the testing capability of wind tunnels was always a priority. The efficiency of data acquisition, as well as data accuracy are of great importance. One of the main ways of improving data accuracy is to eliminate the wall interference. Over time, several correction methods have been developed, the first being those that use theoretical, idealized boundary conditions, followed by methods that use measured boundary conditions. The purpose of this paper is to determine the perforated wall corrections using the one-variable method and measured boundary pressures, for the ONERA M4R calibration model.

Keywords: wind tunnel, perforated wall interference, ventilated walls, pressure bounday measurements.

1. Introduction

In order to assess the wall interference problem in a wind tunnel, several methods have been developed. These include methods based on the rotational non-viscous flow hypothesis or the viscous fluid hypothesis, but the most commonly used are the ones based on the potential flow hypothesis [1]. Their main advantage is given by the fact that they have a simple shape and, implicitly, a high computation speed. The results obtained using potential flow methods are accurate as long as the model is relatively small compared to the test section.

It was demonstrated both experimentally and by means of computational techniques, that the characteristic properties of the flow through the perforations of a ventilated wall are dependent on the boundary layer [1]. However, this has not prevented the development of various correction methods based on idealized boundary conditions. The most significant advantage of using this type of boundary conditions is the necessity to only measure the parameters that are directly related to the model tested in the wind tunnel. However, the importance of measured boundary conditions has long been recognized, due to the fact that they describe more accurately the behaviour during the experiments. The difference between the

[1] INCAS – National Institute for Aerospace Research "Elie Carafoli", Bd. Iuliu Maniu 220, Bucharest 061126, Romania
[2] PhD student, University POLITEHNICA of Bucharest, Romania
[*] Corresponding author: Mihaela BURGHIU (MANEA), E-mail: manea.mihaela@incas.ro

theoretical approach and the use of the experimentally obtained boundary conditions, consists in replacing the idealized boundary condition with the measured one.

The one-variable method is probably the most widely used technique in the assessment of wall interference that uses boundary pressure measurements, because it only requires the measurement of a single variable, the streamwise component of the interference velocity. The basic assumption of this method is that the potential near the walls is governed by the Prandtl-Glauert equation.

$$\frac{\partial^2 \varphi}{\partial x^2} + \frac{\partial^2 \varphi}{\partial y^2} + \frac{\partial^2 \varphi}{\partial z^2} = 0 \tag{1}$$

By differentiating the potential φ with respect to x, the streamwise component of the perturbation velocity, u, can be determined. Using the linear superposition, u can be represented as [2] [3] [4]:

$$u = u_{\mathrm{M}} + u_{\mathrm{W}} \tag{2}$$

where u_{M} is the streamwise component of the disturbance potential of the model placed in an infinite free stream and u_{W} is the streamwise component of the wall interference potential.

In order to compute the wall interference at high subsonic Mach numbers it is necessary to apply a compressibility correction. This can be achieved by introducing the Prandtl Glauert compressibility factor, β [5], which converts the original coordinate system, defined by (x, y, z) in a coordinate system defined by $(\tilde{x}, \tilde{y}, \tilde{z})$, where:

$$\tilde{x} = \frac{x}{\beta}, \quad \tilde{y} = y, \quad \tilde{z} = z \tag{3}$$

$$\beta = \sqrt{1 - M^2} \tag{4}$$

As indicated in [2], u_{W} satisfies the Laplace equation in the entire test section.

$$\frac{\partial^2 u_{\mathrm{W}}}{\partial x^2} + \frac{\partial^2 u_{\mathrm{W}}}{\partial y^2} + \frac{\partial^2 u_{\mathrm{W}}}{\partial z^2} = 0 \tag{5}$$

Free air velocity can be computed if the model is represented by singularities.

$$u_W = u - u_M = -\beta \left(\frac{1}{2} Cp + \frac{\partial \varphi_M}{\partial x} \right) \tag{6}$$

The pressure coefficient, Cp, is computed using the boundary pressure measurements. If the walls are sufficiently remote from the model, only the far field aproximation of u_M is necessary.

This paper presents the assessment of the primary perforated wall corrections using a panel method.

2. Wall interference computation

Equations (2) and (5) describe an interior Dirichlet problem, for which there are several methods of solutioning. The Dirichlet problem stated for Laplace equation, to which equation (5) can be reduced, has a unique solution in the interior of a region , provided that the boundary conditions are specified at any point on the surface. If the interference potential is specified on the surface, it is necessary to define an appropriate Green function, that vanishes on the surface, leaving:

$$4\pi\varphi_W(p) = \int (\varphi - \varphi_M)\frac{\partial G_D}{\partial n} dS \tag{7}$$

Once the Green function, G_D, is defined, and if the perturbation velocity potentials are known over the entire surface, the above integral can be evaluated [6].
As stated in [7], u_W can be represented by using the double layer potential.

$$u_W(r_0) = \iint I(r)\frac{\partial}{\partial n}\left(\frac{1}{4\pi|\vec{r}_0 - \vec{r}|}\right) dS \tag{8}$$

where I is the doublet density, S is the test section surface and the position vectors $\vec{r}_0 = (\tilde{x}_0, y, z)$ and $r = (\tilde{x}, y, z)$ define a fixed observation point and a point running over the test section surface.

As $\vec{r}_0$ approaches a smooth surface point $\vec{r}_k$, u_W can be described by using Fredholm integral of the second kind for the doublet strength [2].

$$u_w(\vec{\mathrm{r}}_\mathrm{k}) = -\frac{1}{2}I(\vec{\mathrm{r}}_\mathrm{k}) + \iint I(\vec{r})\frac{\partial}{\partial n}\left(\frac{1}{4\pi|\vec{\mathrm{r}}_\mathrm{k} - \vec{r}|}\right) dS \tag{9}$$

The wind tunnel test section is divided in rectangular panels. The model is represented by using singularities. Thereby, the disturbance velocity potential induced by the wing is aproximated by a discrete distribution of 20 horseshoe vortices placed on the quarter chord line, the fuselage is represented by a distribution of 8 three dimensional doublets placed on the fuselage axis, and the wake effect is aproximated by a point source placed on the trailing edge.

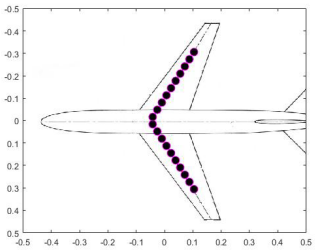

Fig. 1: Horseshoe vortices distribution

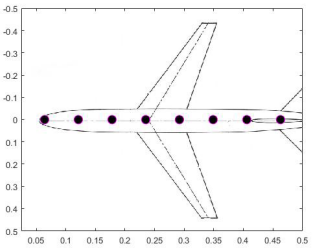

Fig. 2: Three dimensional doublets distribution

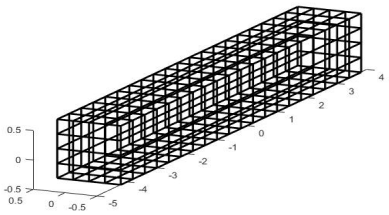

Fig. 3: Test section representation

The potentials describing the representations mentioned above are:

$$\varphi_M^A = \frac{\Gamma}{4\pi}\frac{z}{y^2+z^2}\left(1+\frac{x}{\sqrt{x^2+y^2+z^2}}\right) \tag{10}$$

$$\Gamma = \frac{1}{2}SC_L \tag{11}$$

$$\varphi_M^S = \frac{d}{4\pi}\frac{x}{(x^2+y^2+z^2)^{3/2}} \tag{12}$$

$$d = V \tag{13}$$

$$\varphi_M^D = \frac{-\sigma}{4\pi}\frac{1}{(x^2+y^2+z^2)^{1/2}} \tag{14}$$

$$\sigma = \frac{1}{2}SC_D \tag{15}$$

where φ_M^A describes the wing, φ_M^S describes the fuselage and φ_M^D describes the wake. Γ, d and σ are the singularities strengths, V is the fuselage volume, S is the reference surface, C_L is the lift coefficient and C_D is the drag coefficient.

$$\varphi_M = \varphi_M^A + \varphi_M^S + \varphi_M^D \tag{16}$$

If the test section is divided into N rectangular elements and $\vec{r}_k$ is positioned at the centroid of each element, the following linear system results:

$$\sum_{j=1}^{N} A_{kj} I_j = u_k, \quad k = 1, \dots, N \tag{17}$$

$$A_{kj} = \begin{cases} -\frac{1}{2}, & j = k \\ \iint \frac{\partial}{\partial n}\left(\frac{1}{4\pi|\vec{r}_k - \vec{r}|}\right) dS, & j \neq k \end{cases} \tag{18}$$

After the determination of doublet strengths, u_w can be computed at any point in the test section.

The blockage interference factor and the angle of attack correction are computed as [2]:

$$\varepsilon(x,y,z) = \frac{1}{\beta} u_w(\tilde{x},y,z) \tag{19}$$

$$\Delta\alpha_z(x,y,z) = \int_{\tilde{x}_R}^{\tilde{x}} \frac{\partial u_W}{\partial y}(\tilde{x},y,z)d\tilde{x} - \frac{\partial \varphi_M}{\partial y}(\tilde{x}_R,y,z) \tag{20}$$

where $\tilde{x}_R$ is the coordinate of the reference plane.

The blockage in the test section influences the free air velocity, therefore it is necessary to correct the reference flow quantities, such as Mach number and dynamic pressure. For a small ε and $\gamma = 1.4$, the liniarized corrections are presented below [8]:

$$M_\infty = M \cdot [1 + (1 + 0.2M^2)\varepsilon] \tag{21}$$

$$q_\infty = q \cdot [1 + (2 - M^2)\varepsilon] \tag{22}$$

3. Boundary pressure measurements

The experiments in which the pressure distributions on the test section perforated walls were measured were performed in the INCAS Trisonic wind tunnel, using the ONERA M4R model. The tunnel is equipped with a perforated wall test section measuring 1.2 x 1.2 meters. The porosity of the walls can be varied between 1.5% and 9.1%. The length of the test section is about 4 meters and the perforations are inclined at 60^0 and their diameter is 10 mm.

ONERA M4R is part of ONERA calibration models family and has a typical transonic transport configuration. The wings have a 30^0 sweep, a 7.31 aspect ratio and a taper ratio of 0.3. Both wing and tail airfoils have a 'peaky' type symmetric cross section [9] [10]. The main dimensions for ONERA M4R model are: 0.635 m wing span, 0.0889 m mean aerodynamic chord, 0.05516 m^2 wing surface, 0.684 m fuselage length and 0.08033 m fuselage diameter [11].

Fig. 4: INCAS Trisonic wind tunnel perforated walls test section

Fig. 5: ONERA M4R model

Boundary pressure measurements were performed by using two cylindrical probes, placed on the top and bottom walls of the test section.

The tip of the probe has the shape of a cone with a semi-angle of 10^o. The tip is followed by a cylinder with a 28 mm diameter and 3200 mm length. The probe was fixed on the wall using 14 mounting brackets and M4 screws. On the probe are installed 44 pressure taps, from which only 32 were used in this experimental campaign.

At the same time with pressure measurements, aerodynamic loads and flow parameters measuremets were also performed. A base pressure correction was applied to the measured data. The experiments evaluated in this paper are presented in the next table.

Table 1

Experiments with ONERA M4R

Experiment Number	Mach number	Roll angle [deg]	Total Pressure [bar]	Angle of attack sweep [deg]
10101	0.5	0	1.4	-8;+10
10102	0.7	0	1.8	-8;+10
10103	0.85	0	1.6	-5;+15

The main source of inaccuracy in the boundary pressure measurements based methods for determining the wall interference is the limited number of pressure measurements. It is necessary to interpolate or extrapolate the existing data in order to be able to define the boundary conditions on the entire domain and to solve the Dirichlet problem. The computations performed for this paper required that u_I to be known at the center of each rectangular element and therefore the measured pressure coefficients were interpolated using spline interpolation. The restricted number of measured pressures and also the lack of measurements for upstream and downstream portions of the domain are the main reasons why the corrections are only aproximate. The pressure coefficients were computed using the formula presented below.

$$C_p = \frac{p - p_s}{q}\ ,\ \ q = \frac{\gamma}{2} p_s M^2 \tag{23}$$

where p is the measured pressure, p_s is the static pressure, q is the dynamic pressure, $\gamma = 1.4$ is the specific heat ratio and M is the flow Mach number. A regular case of pressure distributions is presented in Fig. 6. Also, Fig. 7 displays an exemple of interpolated pressures on top and bottom walls of the wind tunnel.

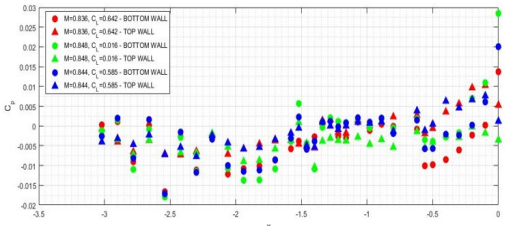

Fig. 6: Pressure distributions exemple for M=0.85

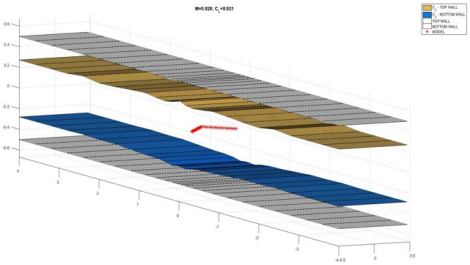

Fig. 7: Interpolated pressure distributions on top and bottom walls

4. Results

In order to to correct the data obtained during experiments, the upflow and blockage corrections factors for ONERA M4R were computed using the procedure described in previous chapters. First, the angle of attack is corrected with the upflow angle, $\Delta\alpha$. Next, the Mach number is corrected using the blockage factor, ε. The change in the Mach number influences the dynamic pressure, therefore a correction of measured aerodynamic coefficients is also necessary. A comparison between uncorrected and corrected lift and drag coefficients for 0.5, 0.7 and 0.85 Mach numbers is presented in this chapter.

For the case of M=0.5 the lift coefficient is compared with the results obtained by Mokry for the ONERA M5 model in the 5ft. × 5 ft. NAE wind tunnel, at a Mach number of 0.505. However, it must be mentioned that the results in [12] are corrected only with the lift interference.

The results for M=0.7 and M=0.85 are compared with those from [13], obtained for the ONERA M5 model placed in the 2m × 2m JAXA Transonic Wind Tunnel. The wall corrections in [13] were determined by applying Mokry's method to the experimental data and are also taking into account the model support interference.

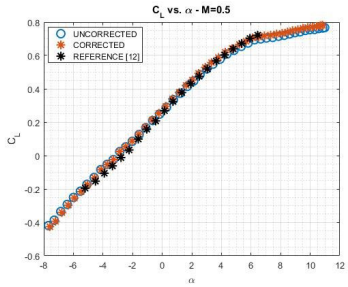

Fig. 8: Corrected vs. uncorrected lift coefficient, M=0.5

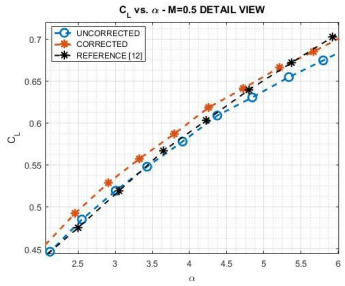

Fig. 9: Corrected vs. uncorrected lift coefficient, M=0.5, detail view

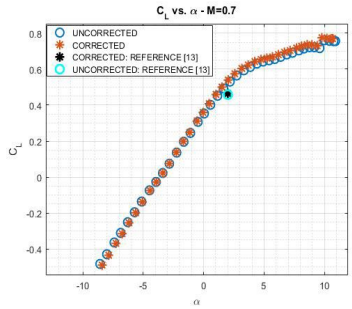

Fig. 10: Corrected vs. uncorrected lift coefficient, M=0.7

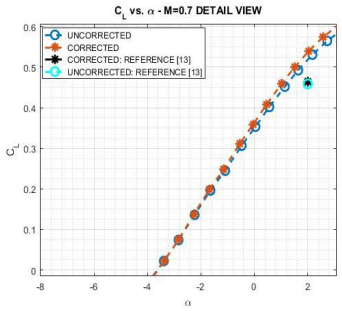

Fig. 11: Corrected vs. uncorrected lift coefficient, M=0.7, detail view

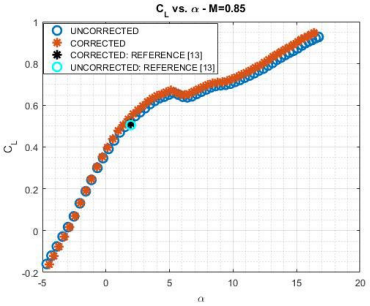

Fig. 12: Corrected vs. uncorrected lift coefficient, M=0.85

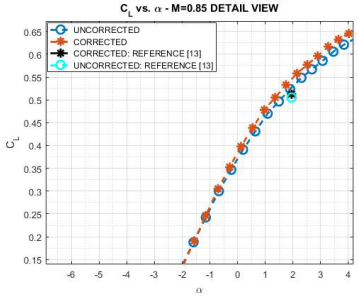

Fig. 13: Corrected vs. uncorrected lift coefficient, M=0.85, detail view

The curves in Fig. 8 to Fig. 13 display the corrected lift coefficient as a function of corrected angle of attack and the unccorrected lift coefficient as a function of uncorrected angle of attack.

It can be observed that the magnitude of lift coefficient corrections increases as the angle of attack increases. For angles of attack higher than 8 degrees its value is very high, being situated between -0.011 and -0.014. Also, the lift coefficient corrections increase with increasing Mach number.

In the case of M=0.5 it can be noticed that the corrected results seem to be comparable with those of Mokry, even though the latter have only the lift interference correction applied.

Both corrected and uncorrected results for M=0.7 and M=0.85 do not perfectly fit the results obtained in the JAXA wind tunnel, but it can be seen that the corrected ones have the same tendency as the ONERA M5 results. For an angle of attack of aproximately 2^0, the relative error between corrected and uncorrected lift coefficient for ONERA M5 is 1.2% at M=0.7 and 1.46% at M=0.85 while for ONERA M4R is 1.5% at M=0.7 and 1.7% at M=0.85. The differences may occur due to the fact that the two models are not identical, they were tested in two different wind tunnels and also the results presented in this paper do not take into account the model support interference. Moreover, the magnitude of ONERA M4R corrections is higher than the magnitude of the ONERA M5 corrections. This could

be explained by the fact that the blockage caused by the ONERA M4R in the INCAS trisonic wind tunnel is higher than the blockage caused by ONERA M5 in JAXA wind tunnel, therefore resulting that the test section walls influence on M4R is more significant than that on M5.

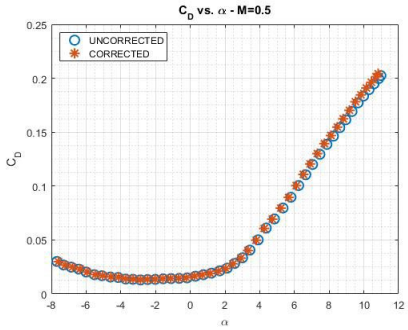

Fig. 14: Corrected vs. uncorrected drag coefficient, M=0.85

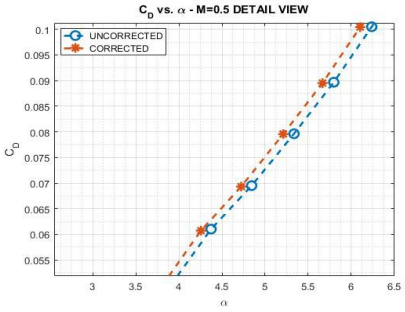

Fig. 15: Corrected vs. uncorrected drag coefficient, M=0.85, detail view

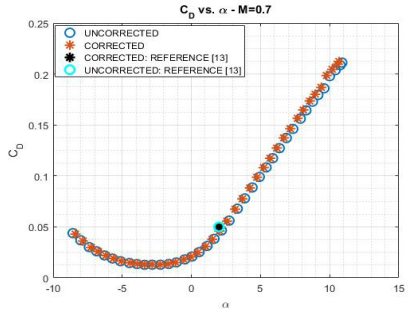

Fig. 16: Corrected vs. uncorrected drag coefficient, M=0.85

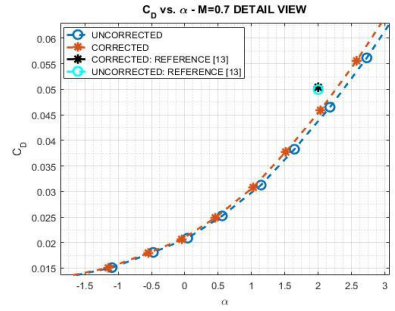

Fig. 17: Corrected vs. uncorrected drag coefficient, M=0.85, detail view

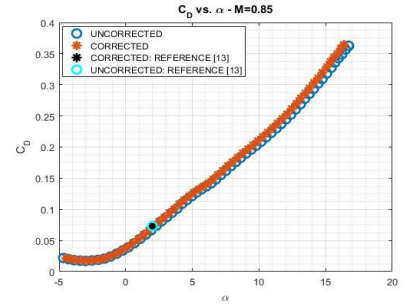

Fig. 18: Corrected vs. uncorrected drag coefficient, M=0.85

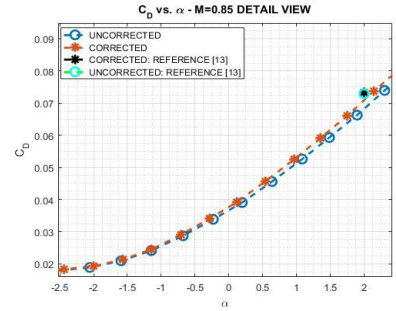

Fig. 19: Corrected vs. uncorrected drag coefficient, M=0.85, detail view

The drag coefficient is presented in a similar way with the lift coefficient in Fig. 14 to Fig. 19. Also, it shows the same tendency as the lift coefficient, increasing as the angle of attack increases.

At aproximately 2^0 angle of attack, the relative error between corrected and uncorrected drag coefficient for ONERA M5 is 0.93% at M=0.7 and 0.6% at M=0.85 while for ONERA M4R is 1.3% at M=0.7 and 0.7% at M=0.85. Regarding the comparison with the results from [13], it can also be noticed that there are differences between the two sets of data, but the possible reasons for the appearance of these differences are explained above.

5. Validation of corrections

Concerning the validation of corrections determined in this paper, the method used in [14] is applied. In this reference, the autor uses a theoretical wall pressure distribution generated by a porous wall boundary condition interference prediction method as a benchmark test to asses the corrections obtained using the one-variable method.

Similarly, in this paper, the pressure distributions on the walls were generated using the method described in [15] [12]. Also, by applying the same method, the angle of attack correction was computed for ONERA M4R model, 0.7 Mach number. Next, the generated pressure distributions were used as 'measured' input for the method presented in this paper. Having the boundary conditios defined, it was easy to compute the angle of attack correction.

The pressure coefficients, C_p, were determined from the theoretical boundary conditions by applying the liniarized equation [12]:

$$C_p = -2\frac{\partial \varphi}{\partial x} \tag{24}$$

The results are presented in Fig. 20. Even though there are differences between the two sets of corrections, they are in general below 10% and may occur due to the differences in computation of corrections between the two methods. In the first method, that uses a porous wall condition, the test section is assumed to be infinitely long, while in the second method the test section is limited by upstream and downstream boundary conditions.

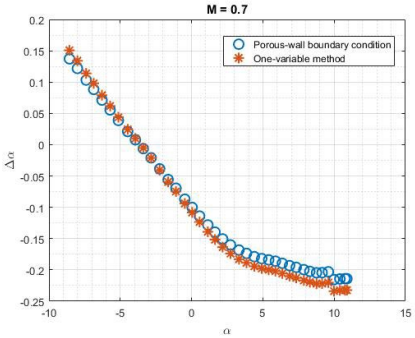

Fig. 20: Angle of attack correction computed using two methods – M=0.7

Another way to verify the corrections, used for NASA TWICS correction system is presented in [16]. Although the method is applied for slotted wall interference, it can be assumed that it is also valid for perforated wall interference.

Mach number and angle of attack corections are represented as a function of uncorrected angle of attack. In the case of the Mach number, the corrections should be negative throughout the entire domain, having a value that increases with increasing incidence. In the case of angle of attack correction, the curves are expected to be liniar if no flow separation region appears. Also, they should have a negative slope.

As it can be seen in Fig. 21 and Fig. 22, Mach number and angle of attack corrections fall within the requirements specified above.

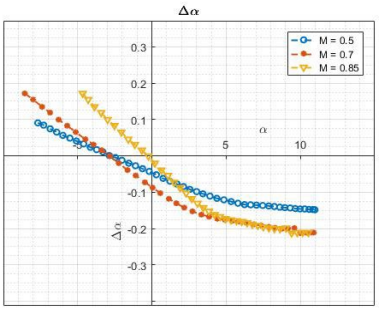

Fig. 21: Angle of attack correction as a function of uncorrected angle of attack

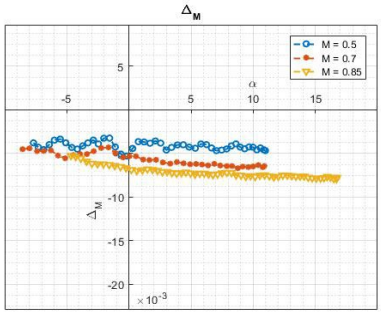

Fig. 22: Mach number correction as a function of uncorrected angle of attack

6. Conclusions

The purpose of this paper was to determine the primary perforated wall corrections for the ONERA M4R model placed in INCAS Trisonic Wind Tunnel by using boundary pressure measurements. The corrections were computed using the one variable method, developed by Mokry in [7] for a half-model placed in a rectangular test section. The results obtained for the case of a full-model were computed using the pressures measured with only two probes placed on the wind tunnel walls.

As expected, the magnitude of corrections for lift and drag coefficients show a significant increase as the angle of attack and Mach number increase.

The corrections were validated by computing 'artificial' pressure distributions and using them as inputs for one variable method.

The accuracy of one variable method is dependent on the accuracy of wall pressure measurements and also on the accuracy of model representation. Even though the use of only two pressure probes could lead to less accurate results, the corrections seem to fall within the expected results.

The use of singularities becomes problematic at high angles of attack, when the flow separation regions are not precisely known, and also at high Mach numbers, when supersonic flow regions might appear.

R E F E R E N C E S

[1] *E. B.F.R.*, "Wind Tunnel Wall Correction," Canada Communication Group Inc., Quebec, 1998.

[2] *M. Mokry*, "Subsonic Wall Corrections in the IAR 1.5 m Wind Tunnel," Institute forAerospace Research, Ottawa, 2006.

[3] *C. B. F. M. J. W. A. Toledano*, "Improvement of Subsonic Wall Corrections in an Industrial Wind Tunnel," in *CASI 62nd Aeronautics Conference*, Montreal, 2015.

[4] *F. M. J. W. A. Toledano*, "Improvement of Wall-Corrections at the National Research Council's Trisonic Wind Tunnel," *Journal of Aircraft,* vol. 56, no. 6, 2019.

[5] *N. Ulbrich*, "Description of Panel Method Code ANTARES," Ames Research Center, California, 2000.

[6] *P. Ashill, J. Hackett, M. Mokry and F. Steinle*, "Boundary Measurements Methods," AGARD, 1998.

[7] *M. Mokry and J. P. R. Digney,* "Doublet-Panel Method for Half-Model Wind-Tunnel Corrections," *Journal of Aircraft,* 1987.

[8] *C. Nae and O. Trifu,* "Analiza Comparativa a Eficientei Procedurilor CFD pentru Determinarea Corectiilor de Pereti (Comparative Analisys of CFD Efficiency in Wall Interference Assessement)," INCAS, Bucuresti, 2001.

[9] *F. Munteanu,* "Experiments with ONERA M4R," INCAS Internal Report, Bucharest, 2012.

[10] *M. S. S. M. C. C. A. R. R. S. M. L. C. C. Reis*, "Aerodynamic Loads Acting on the M5/ONERA/IAE Aeronautical Standard Model," *Journal of Physics,* 2019.

[11] *D. V. G. O. B. I. B. R. D. Damljanovic,* "Wind Tunnel Testing of ONERA-M, AGARD-B and HB-2 Standard Models at Off-Design Conditions," *Aerospace,* vol. 8, no. https://doi.org/10.3390/aerospace8100275, 2021.

[12] *M. Mokry and R. Galway,* "Analysis of Wall Interference Effects on ONERA Calibration Models in the NAE 5-ft. Wind Tunnel," NRC Aeronautical Report, Ottawa, 1977.

[13] *M. K. A. Hashimoto,* "Wall Interference Analysis by Whole Wind Tunnel CFD," in *5th Symposium on Integrating CFD and Experiments in Aerodynamics*, Tokyo, 2012.

[14] *M. Mokry*, "Theory of Subsonic Wall Interference in a Cylindrical-Boundary Wind Tunnel Revisited," in *AIAA*, 2001.

[15] *A. B. M. Manea,* "Lift Interference in Wind Tunnels with Perforated and Solid Walls," *INCAS Bulletin,* vol. 13, no. 1/2021, 2021.

[16] *N. Ulbrich,* "Wall Interference Correction System of the NASA Ames 11-ft Transonic Wind Tunnel," California.